Abstract: For a Nd:YVO_4 crystal, a strong thermal lens astigmatism is observed by using a probe beam technique. By orienting the c-axis of the Nd:YVO_4 crystal in the tangential plane of the ring resonator, we find the two astigmatisms introduced by the ring cavity and thermal lens can be mutually compensated. Such compensation improves the stability, beam quality, and conversion efficiency of the laser. As a result, a single-frequency green laser of 25.3 W ($M^2 < 1.10$) was obtained with an optical-optical conversion efficiency of 32.2%, and the power stability is better than $\pm 0.4\%$ over 8 hours. To the best of our knowledge, this is the highest output power and conversion efficiency of intracavity frequency-doubling single frequency green Nd:YVO_4 laser.

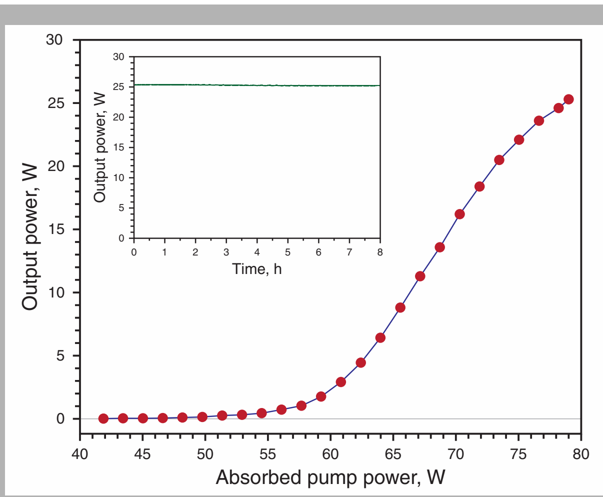

Laser output power *versus* pump power and power stability in 8 hours

High-power single-frequency Nd:YVO_4 green laser by self-compensation of astigmatisms

Y.J. Wang, Y.H. Zheng, * *Z. Shi, and K.C. Peng*

State Key Laboratory of Quantum Optics and Quantum Optics Devices, Institute of Opto-Electronics, Shanxi University, Taiyuan 030006, China

Received: 7 March 2011, Revised: 9 April 2012, Accepted: 15 April 2012
Published online: 11 June 2012

Key words: thermal lens astigmatism; ring cavity; self-compensation, direct pumping

1. Introduction

High power single frequency solid-state green lasers can be used for a variety of roles, such as pumping of Ti:Sapphire or dye lasers, precision measurement, and high-resolution laser spectroscopy. In the past 20 years, extensive efforts had been made for producing high power single frequency green lasers. In the 1990s, watt-level single frequency green lasers were obtained by single-end pumping, with the highest output power of 3.2 W and optical-optical efficiency of 25.4% [1–3]. Recently, the coherent Inc. designed and built a commercial single frequency 532 nm lasers, which highest output power is 18 W corresponding to an optical-optical conversion efficiency of 25% [4]. However, the power scaling and beam quality are limited by thermal effects of the gain medium. Mitigating and compensating the thermal effects have been the focus of the study of high-power lasers. Mitigating the thermal effect can be accomplished by a composite gain medium [5,6], low-doped gain medium [7], dual-end pumping and direct pumping [8–10]. The thermal effects of the gain medium can be approximated with an equivalent lens. The real thermal lens is not an ideal thin lens but a lens including the aberrations of spherical and astigmatism [11,12], thus the compensation of the thermal lens astigmatism (TLA) is complicated.

Some techniques have been used to compensate the TLA, such as inserting a cylindrical intracavity element

* Corresponding author: e-mail: yhzhengsxu@hotmail.com, yhzheng@sxu.edu.cn

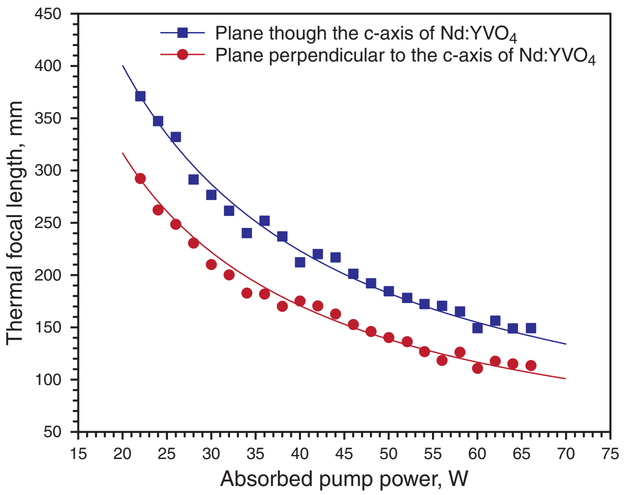

Figure 1 (online color at www.lasphys.com) Measured thermal focal lengths at different pump powers, which show the thermal lens astigmatism

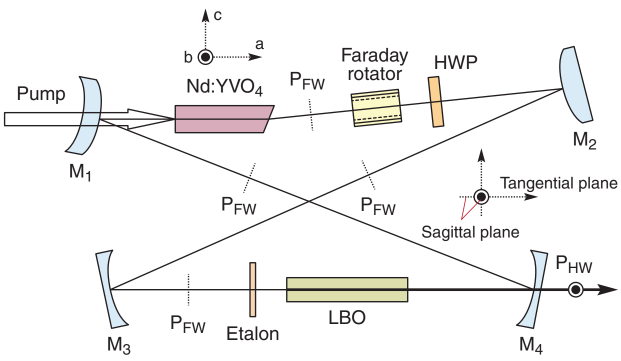

Figure 2 (online color at www.lasphys.com) Experimental setup of the single-frequency green laser. TGG – terbium gallium garnet, HWP – half wave plate, LBO – lithium triborate, P_{FW} – polarization direction of the fundamental wave, and P_{HW} – polarization direction of the harmonic wave

into the cavity [13], tilting the intracavity lens [14], and using two rods with orthogonal c-axes [15,16] in a linear cavity. However, these designs require additional optical elements and make the laser alignment more troublesome.

In this letter, with a 888 nm laser diode as the pump source of a high power single frequency Nd:YVO_4 green laser, the thermal effects in the pumping process were mitigated greatly. By orienting the c-axis of the Nd:YVO_4 crystal in the tangential plane (horizontal to optical table) of the ring cavity, the astigmatisms introduced by the thermal lens and the ring cavity can be mutually compensated. Due to the mitigation and compensation of the thermal effects, the single-frequency laser can be scaled up to a higher output power whilst retaining the excellent performance at low power, a 25.3 W high power intracavity frequency-doubling single-frequency green laser was obtained with 32.2% of the optical-optical conversion efficiency. To the best of our knowledge, this is the highest output power and conversion efficiency of intracavity frequency doubling single frequency green Nd:YVO_4 laser. The power stability of the green laser at 25.3 W is better than ±0.4% over 8 hours.

2. Thermal character analysis of the laser crystal

Thermal lens is a critical factor for resonator design, and must be thoroughly considered and characterized if an optimum design for efficient lasing operation is to be achieved. In order to quantify the influence of the thermal effects and find an optimal resonator scheme, the value of the thermal focus in Nd:YVO_4 crystal is measured by a probe beam technique [13]. A linearly polarized beam (probe beam) is carefully aligned to propagate collinearly with the pump beam through the Nd:YVO_4 crystal, and then directed to a M^2 meter. By measuring the waist position of the probe beam with and without the pump light injecting into the Nd:YVO_4 crystal, we can calculate the thermal focal length f_{th} based on the expression $f_{th}=-2f^2/\Delta x$ [13], where f is the focus of the lens at the front of the M^2 meter, Δx is the difference between the final waist positions with and without the thermal lens.

We adjust the polarized direction of the probe beam parallel to the c-axis of Nd:YVO_4 crystal (the polarized direction of the oscillation light), and measure the thermal focal length in two planes (including perpendicular to the c-axis and parallel to the c-axis of Nd:YVO_4 crystal) as a function of the pump power, respectively. Fig. 1 shows the measured results, and it can be seen that a strong astigmatism of the thermal lens was observed. Here circles and squares correspond to the thermal focal length perpendicular and parallel to the c-axis of Nd:YVO_4 crystal, respectively, and the solid lines are fitting results. The TLA affects severely the laser performance and must be considered to optimize the resonator design.

3. Experimental setup and analysis

A fiber coupled laser diode (LIMO Inc., LIMO-F400-DL888-EX1458), with the highest output power of 90 W and central wavelength of 888 nm, is used as the pump source. The coupling fiber has a core diameter of 400 μm with a N.A of 0.22. A pump wavelength of 888 nm is preferred to 808 nm owing to the two reasons: First, due to the reduced quantum defect of direct laser level pumping, the fractional thermal load mitigates from 24.1% to 16.5% at 1064 nm lasing, which enables higher pump power to inject while does not increase the thermal load of the gain

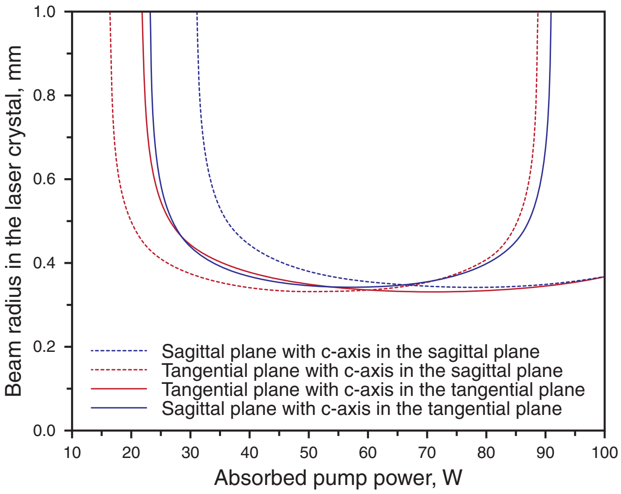

Figure 3 (online color at www.lasphys.com) Stable region and beam radius of the laser, solid line – our design and dotted line – conventional laser

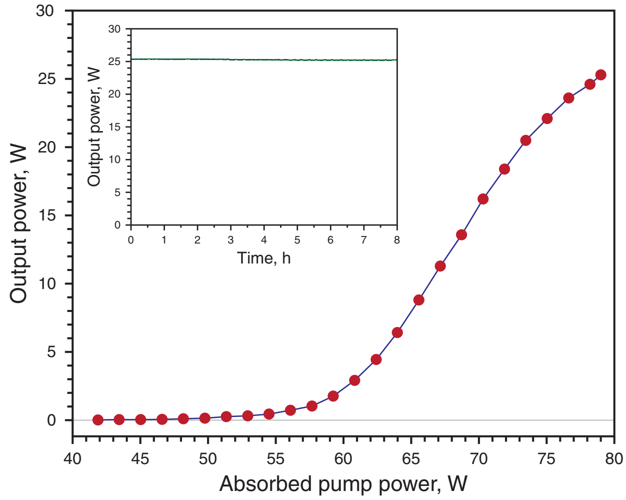

Figure 4 (online color at www.lasphys.com) Laser output power *versus* absorption pump power and power stability in 8 hours

medium. The other is the polarization-independent pumping, which improves the stability of the laser. However, due to the low absorption cross section of Nd:YVO_4 crystal for 888 nm pumping beam, which is only 4% of that for 808 nm pumping transition [9], a gain medium of high Nd-doped level is chosen to increase the absorption efficiency. The laser diode beam is focused into the Nd:YVO_4 crystal by a telescope system with a transmission efficiency of 98%. A composite Nd:YVO_4/YVO_4 crystal, with an Nd-doped of 0.8% and a 3×3mm^2-cross-section and 23-mm-length (3 mm undoped and 20 mm Nd-doped), serves as the gain medium with an absorption efficiency of 89%.

Fig. 2 shows the experimental setup of our laser system which consists of two convex mirrors (M_1 – S1, AR 888 nm; S2 – HT 888 nm, HR 1064 nm; and M_2 – S1, HR 1064 nm. R = 1500 mm) and two concave mirrors (M_3 – S1, HR 1064 nm and M_4 – S1, HR 1064 nm, HT 532 nm; S2 – AR 532 nm. R = 100 mm) [17]. An α-cut wedge Nd:YVO_4 crystal (S1, S2 – AR 888 and 1064 nm) is used as the gain medium, with a doped concentration of 0.8% and wedge angle of 1.5 degree. The design of the wedge end-facet serves as a polarized beam splitter to suppress the σ-polarization oscillation and enhance the superiority of the π-polarization mode in the mode competition [18]. An optical diode consisting of a faraday rotator (TGG, terbium gallium garnet) and a half-wave plate enforces the single-frequency operation of the laser [19]. An etalon is inserted into the laser resonator as a spectral filter to narrow the gain bandwidth, which ensures the stable single-frequency operation. A lithium triborate (LBO) crystal (S1, S2 – AR 1064 and 532 nm, a cross section of 3×3 mm^2 and length of 18 mm) is used as the second harmonic generator whose temperature is controlled at the noncritically phase-matching temperature of 149°C with a precision of 0.01°C [20,21]. The spot radius of the lasing beam in LBO crystal is approximately 50 μm. Based on the Smith model of intracavity frequency doubling laser, we calculate the optimal length of the LBO crystal (18 mm) to meet the optimal conversion efficiency [17,22].

Based on the measured results of the thermal lens, there are two optical elements that introduce astigmatic distortions, the thermal lens and ring resonator [23]. The astigmatism means that geometrical beam in the plane perpendicular to the c-axis of Nd:YVO_4 rod behaves differently with that in the plane parallel to the c-axis. To analyze such laser system, it is necessary to consider the mode characteristics and the stable region of the tangential (horizontal to optical table) and sagittal (vertical to optical table) planes of the resonator separately. With the method of ABCD transfer matrix, we analyzed the beam parameters at different planes of the cavity. The analysis results are shown in Fig. 3. In conventional lasers, in order to reduce the losses due to the imperfect reflection for p-polarization beam of the cavity mirrors, the c-axis of the Nd:YVO_4 crystal is usually set to be parallel to the sagittal plane of the ring cavity. However, we can see, from the dotted line of Fig. 3, that the superposition of the two astigmatisms leads to a significant discrepancy of the beam size and stable range in the tangential and sagittal planes.

In our design, by orienting the c-axis of the Nd:YVO_4 crystal in the tangential plane of the ring resonator and optimizing the resonator parameters, the combined action of the two astigmatisms can be mutually compensated, which is clarified from the solid line of Fig. 3. The compensation of astigmatisms not only expands the stability range of the laser, but also reduces the difference of beam size in the tangential and sagittal planes. The wide stable range is advantageous to improve the stability of the laser. The round

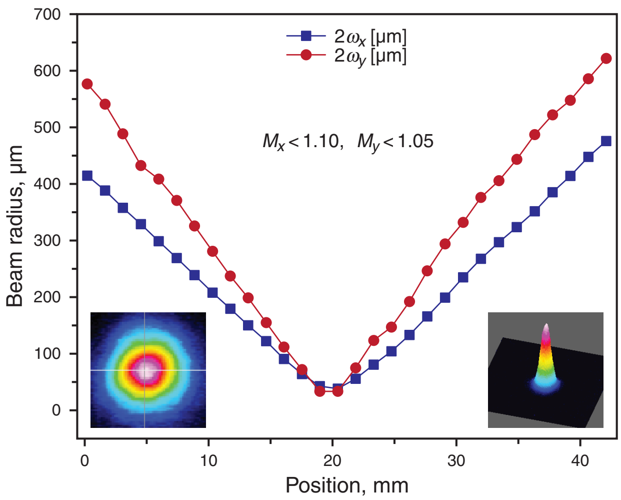

Figure 5 (online color at www.lasphys.com) Measurement of beam quality, spatial beam profile, and intensity distribution

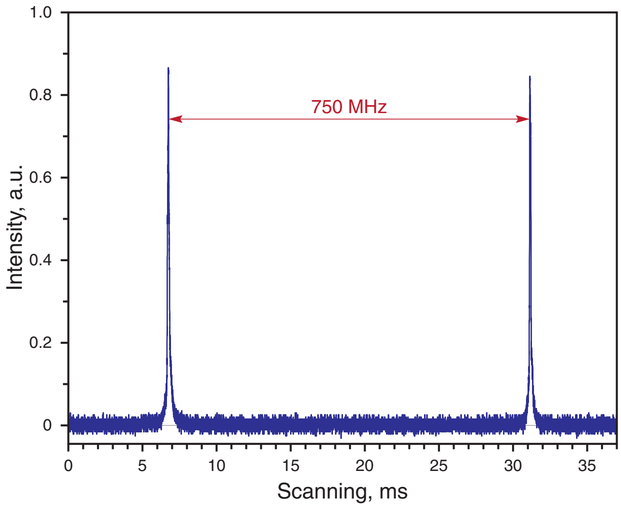

Figure 6 (online color at www.lasphys.com) Scanning confocal Fabry-Perot spectra of the fundamental wave, confirming the single-frequency operation

beam of the fundamental mode makes it easier to obtain a good mode-matching with the pump beam [24], which improves the conversion efficiency of the laser.

4. Experimental results

Under the pump power of 90 W, corresponding to the absorption pump power of 78.5 W, a single-frequency TEM_{00} green laser of 25.3 W was directly measured. The output power *versus* absorption pump power is shown in Fig. 4 (range from laser threshold to 40 W of the absorption pump is omitted), where it is clear that the output power increases monotonously over the whole range of the pump power. The laser threshold is 24.7 W, and the optical-optical conversion efficiency is 32.2% accounting for the transmission and absorption losses of the pump light. The power stability of the green laser at 25.3 W is better than $\pm 0.4\%$ over 8 hours, recorded by a power meter and data acquisition card.

Only when the absorption pump power adjusts from 56.5 to 78.5 W, the output laser mode can keep good beam quality. When the absorption pump power is below 56.5 W, the beam quality becomes worse due to the working point of the laser around the edge of the stability range. At the absorption pump power of 78.5 W, the beam quality of the laser at 25.3 W was measured by a M^2 meter (DataRay Inc.), and the measured values of M_x^2 and M_y^2 are 1.10 and 1.05, respectively. The spatial beam profile and intensity distribution are also shown in Fig. 5.

A Fabry-Perot cavity with a free spectral range (FSR) of 750 MHz and finesse of 200 was employed to monitor the longitudinal mode of the laser. The resolution of 3.75 MHz is enough to distinguish the neighbor longitudinal modes of the laser (the separation of the longitudinal modes is 500 MHz). The measured result is illustrated in Fig. 6 at the highest output power level. It indicates clearly that the laser operates in single-longitudinal mode. Through continuous observation, we find that the laser can maintain stable single-longitudinal operation over 8 hours without mode-hopping.

5. Conclusion

In conclusion, we have observed a strong TLA in $Nd:YVO_4$ crystal. By orienting the c-axis of the $Nd:YVO_4$ crystal in the tangential plane of the ring resonator, the two astigmatisms introduced by the ring cavity and thermal lens can be mutually compensated. At the same time, with a 888 nm laser diode as the pump source, the thermal effect in the pumping process was mitigated greatly. By combining the two methods of direct pumping and self-compensation of astigmatisms, the output power, beam quality, and conversion efficiency of the laser were improved greatly. A high power intracavity frequency-doubling single frequency green laser ($M^2 < 1.10$) was obtained with a maximum output power of 25.3 W and power stability of better than $\pm 0.4\%$ over 8 hours. The optical-optical conversion efficiency is 32.2% with respect to absorption pump power.

Acknowledgements This research is supported by the National High-tech R&D Program of China (2011AA030203), the National Basic Research Program of China (2010CB923101), the National Nature Science Foundation of China (61008001), and the Nature Science Foundation of Shanxi Province (2011021003-2).

References

[1] K.I. Martin, W.A. Clarkson, and D.C. Hanna, Opt. Lett. **21**, 875–877 (1996).

[2] K.I. Martin, W.A. Clarkson, and D.C. Hanna, Appl. Opt. **36**, 4149–4152 (1997).

[3] Y.-F. Chen, T.-M. Huang, C.-L. Wang, and L.-J. Lee, Appl. Opt. **37**, 5727–5730 (1998).

[4] Coherent Web Site http://www.coherent.com/Products/index.cfm?1852/Verdi-V-Series.

[5] J.Q. Zhao, Y.Z. Wang, B.Q. Yao, and Y.L. Ju, Laser Phys. Lett. **7**, 135–138 (2010).

[6] D.Y. Chen, X.D. Li, Y. Zhang, X. Yu, F. Chen, R.P. Yan, Y.F. Ma, and C. Wang, Laser Phys. Lett. **8**, 46–49 (2011).

[7] E. Cheng, D.R. Dudley, W.L. Nighan, Jr., J.D. Kafka, D.E. Spence, and D.S. Bell, US patent 6185235, February 6, 2001.

[8] N. Pavel, T. Dascalu, N. Vasile, and V. Lupei, Laser Phys. Lett. **6**, 38–43 (2009).

[9] L. McDonagh, R. Wallenstein, R. Knappe, and A. Nebel, Opt. Lett. **31**, 3297–3299 (2006).

[10] F. Lenhardt, M. Nittmann, T. Bauer, J. Bartschke, and J.A. L'huillier, Appl. Phys. B **96**, 803–807 (2009).

[11] M. Santarsiero, J. Opt. Soc. Am. A **18**, 1650–1655 (2001).

[12] C. Pfistner, R. Weber, H.P. Weber, S. Merazzi, and R. Gruber, IEEE J. Quantum. Electron. **30**, 1605–1615 (1994).

[13] P.J. Hardman, W.A. Clarkson, G.J. Friel, M. Pollnau, and D.C. Hanna, IEEE J. Quantum. Electron. **35**, 647–655 (1999).

[14] M. Ostermeyer and R. Menzel, Opt. Commun. **160**, 251–254 (1999).

[15] H. Vanherzeele, Appl. Opt. **28**, 4042–4044 (1989).

[16] V.V. Zelenogorskii and E.A. Khazanov, Quantum Electron. **40**, 40–44 (2010).

[17] Y.J. Wang, Y.H. Zheng, C.D. Xie, and K.C. Peng, IEEE J. Quantum. Electron. **47**, 1006–1013 (2011).

[18] Y.H. Zheng, F.Q. Li, Y.J. Wang, K.S. Zhang, and K.C. Peng, Opt. Commun. **283**, 309–312 (2010).

[19] W.F. Zhao, W. Hou, L. Guo, G. Li, X.C. Lin, and J.M. Li, Laser Phys. Lett. **7**, 210–212 (2010).

[20] Y.F. Lü, C.L. Li, X.H. Fu, J. Lu, G.C. Sun, and Z.M. Zhao, Laser Phys. Lett. **7**, 627–629 (2010).

[21] Sh.B. Zhang, Q.J. Cui, B. Xiong, L. Guo, W. Hou, X.C. Lin, and J.M. Li, Laser Phys. Lett. **7**, 707–710 (2010).

[22] R. Smith, IEEE J. Quantum. Electron. **6**, 215–223 (1970).

[23] H. Kogelnik, E. Ippen, A. Dienes, and C. Shank, IEEE J. Quantum. Electron. **8**, 373–379 (1972).

[24] X. Yan, Q. Liu, L. Huang, Y. Wang, X. Huang, D. Wang, and M. Gong, Laser Phys. Lett. **5**, 185–188 (2008).